Electronic Supplementary Information

Fabrication of Well-Aligned TiO$_2$ Nanofibrous Membrane by Modified Parallel Electrodes Configuration with Enhanced Photocatalytic Performance
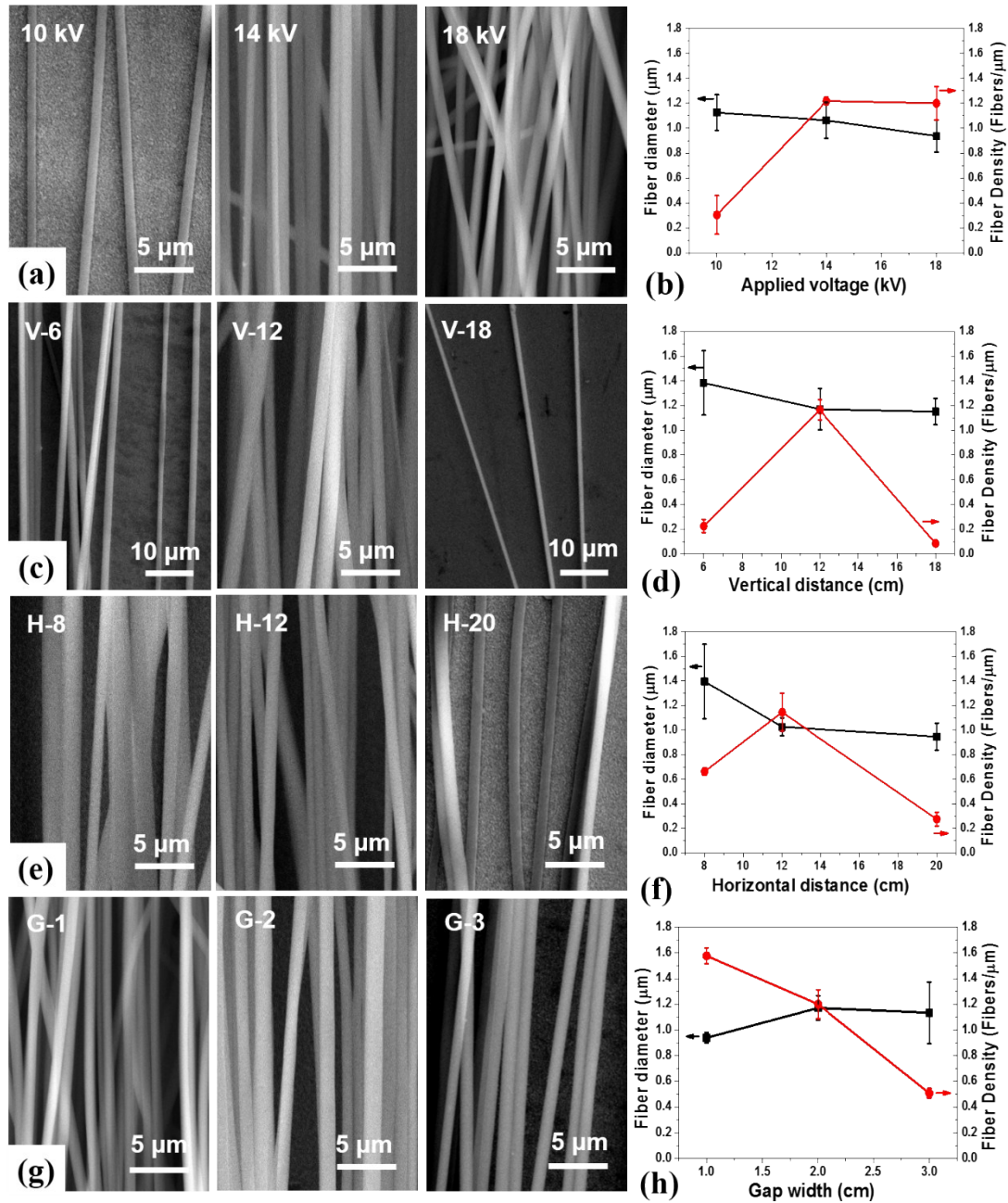
Jianan Wang, Guorui Yang *, Ling Wang, Wei Yan *

Department of Environmental Science and Engineering, State Key Laboratory of Multiphase Flow in

Power Engineering, Xi'an Jiaotong University, Xi'an 710049, China

* Corresponding authors:

E-mail: yanwei@mail.xjtu.edu.cn (W. Yan); yangguorui@mail.xjtu.edu.cn (G. Yang)

Fax: +86-29-82664731.

Fig. S1. SEM images of PVP/A-TiO$_2$ fibers as optimization of electrospinning parameters. Influences of the applied voltages (a) at 10, 14, 18 kV, when V = 12 cm, H = 12 cm, G = 2 cm; spinneret-collector vertical distance (c) of 6, 12, 18 cm, when the 14 kV applied voltages, H = 12 cm, G = 2 cm; collector-assistant electrode horizontal distance (e) of 8, 12, 20 cm, when the 14 kV applied voltages, V = 12 cm, G = 2 cm; and an electrode gap width (g) of 1, 2, 3 cm, when the 14 kV applied voltages, V = 12 cm, H = 12 cm. (b), (d), (f) and (h) The distributions of fiber diameter and fiber density under different electrospinning parameters. All of these tests were conducted under the same collecting time of 1 min.

In Fig.S1, These electrospinning parameters, such as applied voltage, spinneret-collector vertical distance (V), collector-assistant electrode horizontal distance (H) and electrode gap width (G), have been investigated with detail. To quantify the effect degree of parameters, SEM images was taken at three random locations of the same sample and 30 aligned fibers from each sample were measured by
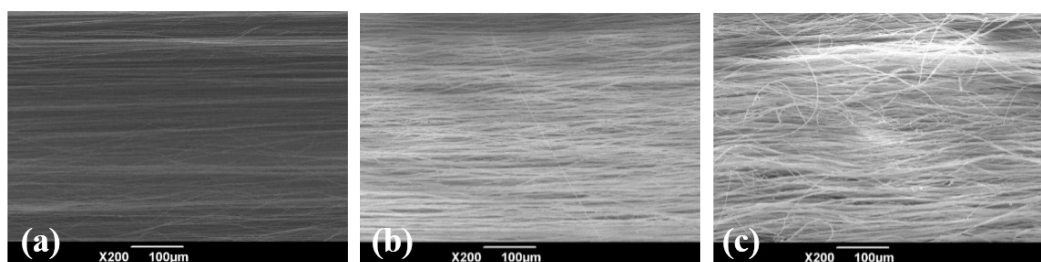
the Image-Pro Plus6.0.

Firstly, different applied voltages were chosen to investigate the degree of fiber alignment and the result was shown in Fig. S1a. When the voltage was lower than 10 kV, the aligned fibers were hardly deposited across the gap, as the electric field force was too low to overcome the viscous force of the solution jet. At a higher voltage of 14 kV, the fibers could be finely formed and exhibited the high degree of alignment. Meanwhile, the fiber diameter stepwise decreased down with the voltage increased (10~18 kV) due to the presence of the enhanced multi-stage unstable tension during electrospinning[1] (Fig. S1b), as well as corresponding to morphological changes from well-aligned fibers to those of less orientation (18 kV). Therefore, the optimum applied voltage was determined to be ~14 kV in our electrospinning system.

The vertical distance between the spinneret and collector plays a crucial role to improve the production and quality of aligned fibers (Fig. S1c, d). If this distance was small (< 6 cm), there was minimal time and space maintaining fibers to reach the collect, and consequently they would fall to the stage. If this distance was longer than 18 cm, the production of aligned fibers was also disappointing as the weaker electric field force with the increased distance was unable to gather the fibers onto the target. However, the longer residence time resulting from the increased distance (6~18 cm) was convenient for the charged fluid to split more times and thus the fiber diameter became smaller. When the vertical distance was ~12 cm, the best fiber production and alignment were achieved.

Similarly, the horizontal distance between collector and assistant electrode in our system also greatly affected the aligned fiber formation (Fig. S1e, f). Different from the coefficient of the electric field force and gravity in the vertical direction, the horizontal movement of fibers just was affected by the electric field force in the horizontal direction. If the distance between collector and assistant electrode was too small (< 8 cm), the fibers would be knocked far away from the gap because of the stronger electric field force. On the contrary, the longer distance (> 20 cm) would lead to a weaker electric field force, which was insufficient for fibers to move to the gap. The gradual decreased fiber diameter could be attributed to the longer residence time likewise. After optimal evaluation, the best quality and production of fibers could be obtained under the H value of ~12 cm.

For the electrospinning collector formed by two parallel electrodes, electrode gap width was deeply associated with the preparation of the aligned fibers. When the gap width was 1 cm, fibers could be fast deposited across the gap but part of them were crooked due to the smaller space impeded the complete stretching of fibers (Fig. S1g). With the increase of gap width, the higher degree of fiber alignment was achieved. However, when the width reached ~3 cm, the production of aligned fibers significantly reduced as the finer fibers could not keep the tensile state and thus were hardly deposited between the two parallel electrodes. This result also provided the explanation of the increased fiber diameter with the gap width increased (Fig. S1h). For this modified electrospinning system, the optimal gap width was confirmed being ~2 cm.

In order to gain the higher production of PVP/ TiO$_2$ aligned fibers, the maximum collection time was investigated. As shown in Fig. S2, the PVP/ TiO$_2$ fibers exhibited an improved production with the collection time increased, and simultaneously the high orientation of fibers was maintained within 5 min. However, when the collection time increased to 10 min, the degree of alignment lowered significantly due to the overloaded fibers across the gap weakened the electrostatic tensile between the two parallel negative electrodes. Thus, the maximum collection time for PVP/ TiO$_2$ aligned fibers was fixed at 5 min.
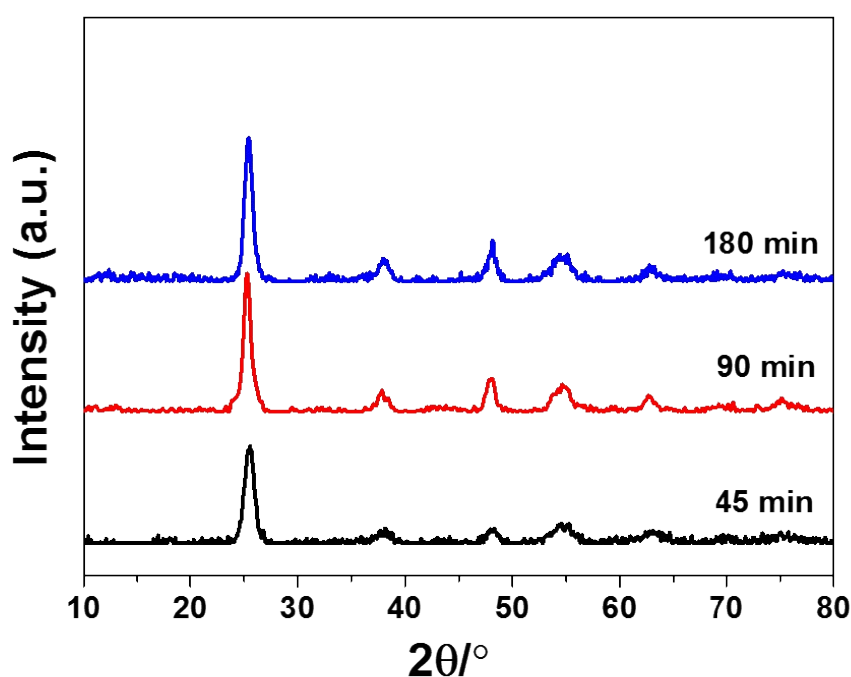
Fig. S3. X-ray diffraction of the sample A-TiO$_2$ under 550 °C for different calcining time.

According to the XRD data in Fig S3, the Debye Scherrer analysis[2] of the full-width at half maximum (FWHM) of the first three strongest peak was used to define the mean particle size of the as-prepared samples:

$$D = \frac{0.89\lambda}{\beta \cos(\theta)}$$

（1）

D is the domain size to be determined, λ is the wavelength of the X-ray, β is the FWHM of the diffraction peak of interest and θ is the angle of the corresponding diffraction peak. Therefore, the particle size of A-TiO$_2$ under 550 °C for 45 min, 90 min and 180 min is calculated to be 9.8 nm, 11.4 nm and 12.5 nm, respectively. This results demonstrate prolonging the calcining time is conducive to the growth of particle, further suggesting that the size of the particle can be varied by controlling the

calcining time.

Variables		Alignment	Diameter (μm)	Density (Fibers/μm)
Applied voltage	10 kV	Good	1.13±0.14	0.30±0.16
	14 kV	Good	1.06±0.14	1.22±0.03
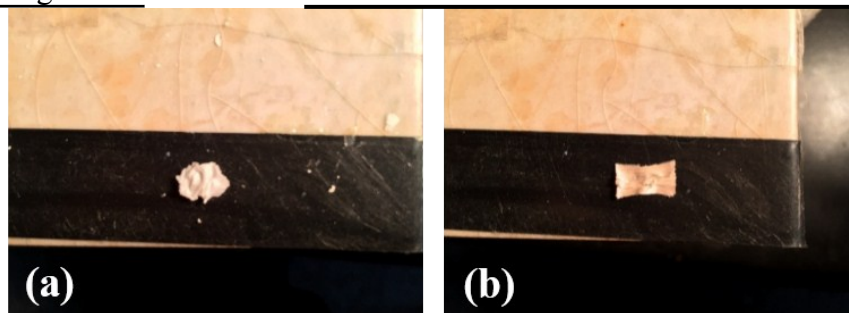
Fig. S4. The images recorded by a camera: (a) N-TiO$_2$; (b) A-TiO$_2$.
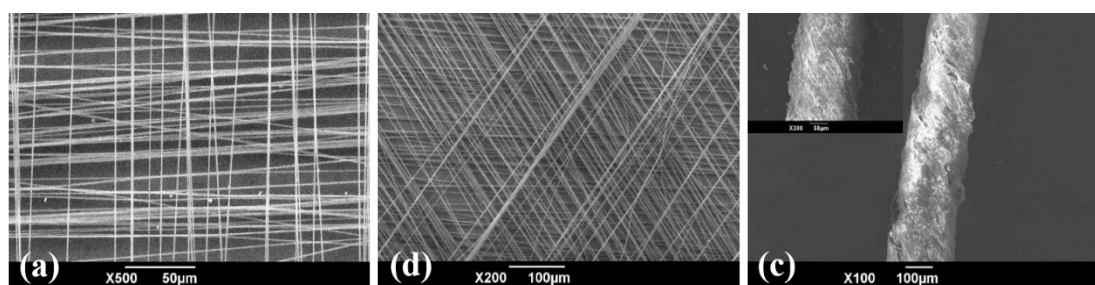
Fig. S5. The SEM images of TiO$_2$ arrayed nanofibers with various patterns: (a) cross; (b) snowflake and (c) sterepsinema.

Table S1. Electrospinning process conditions and their influences on alignment, diameter and density.

			Elements (Atomic %)	
	18 kV	Inferior	0.94±0.13	1.20±0.14
Vertical distance (V)	6 cm	Good	1.38±0.26	0.23±0.05
	12 cm	Good	1.17±0.17	1.16±0.08
	18 cm	Good	1.15±0.11	0.08±0.02
Horizontal distance (H)	8 cm	Medium	1.40±0.3	0.66±0.03
	12 cm	Good	1.02±0.07	1.15±0.16
	20 cm	Good	0.95±0.11	0.27±0.06
Gap width (G)	1 cm	Medium	0.94±0.04	1.58±0.06
	2 cm	Good	1.17±0.09	1.20±0.11
	3 cm	Good	1.13±0.24	0.51±0.04
Collection time	1 min	Good	-	-
	5 min	Good	-	-
	10 min	Inferior	-	-

* The current conditions are fixed at the applied voltages of 14 kV, V = 12 cm, H = 12 cm, G = 2 cm and the collection time of 1 min except for the chosen variables.

Table S2. Relative intensity of $ATiO_2$ and $NTiO_2$ calculated from XRD data in Fig. 5b.

*The sample of Standard is from the standard anatase TiO_2 (JCPDS No. 21-1272)

Sample	Relative intensity				
	101	004	200	105	211
$ATiO_2$	100	11.8	25.7	14.0	18.2
$NTiO_2$	100	17.0	43.6	34.8	38.6
Standard	100	20.0	35.0	19.9	19.9

Table S3. Elementary composition of $A\text{-}TiO_2$ and $N\text{-}TiO_2$ from the XPS data.

	Ti	O	C
A-TiO$_2$	22.92	48.83	28.25
N-TiO$_2$	23.99	52.03	23.98

1. A. L. Yarin, S. Koombhongse and D. H. Reneker, *Journal of Applied Physics*, 2001, **89**, 3018.
2. D. T. Klier and M. U. Kumke, *J. Mater. Chem. C*, 2015, **3**, 11228-11238.